



Published in final edited form as:

Neuroscience. 2009 March 3; 159(1): 369–379. doi:10.1016/j.neuroscience.2008.12.022.

Intraspinal sprouting of unmyelinated pelvic afferents after complete spinal cord injury is correlated with autonomic dysreflexia induced by visceral pain

Shaoping Hou, Ph.D.[#], Hanad Duale, Ph.D.[#], and Alexander G. Rabchevsky, Ph.D.^{*}

Spinal Cord and Brain Injury Research Center, Department of Physiology, University of Kentucky, Lexington, KY 40536-0509

Abstract

Autonomic dysreflexia is a potentially life-threatening hypertensive syndrome following high thoracic (T) spinal cord injury (SCI). It is commonly triggered by noxious pelvic stimuli below the injury site that correlates with increased sprouting of primary afferent C-fibers into the lumbosacral spinal cord. We have recently demonstrated that injury-induced plasticity of lumbosacral propriospinal neurons, which relay pelvic visceral sensations to thoracolumbar sympathetic preganglionic neurons, is also correlated with the development of this syndrome. To determine the phenotype of pelvic afferent fiber sprouts after SCI, cholera toxin subunit beta (CTb) was injected into the distal colon 2 weeks post T4 transection/sham to label colonic visceral afferents. After 1 week transport, the lumbosacral spinal cords were cryosectioned and immunohistochemically stained for CTb, the nociceptive-specific marker calcitonin gene-related peptide (CGRP), and the myelinated fiber marker RT97. Quantitative analysis showed that the density of CGRP⁺ afferent fibers was significantly increased in the L6/S1 dorsal horns of T4-transected versus sham rats, whereas RT97⁺ afferent fiber density showed no change. Importantly, CTb-labeled pelvic afferent fibers were co-localized with CGRP⁺ fibers, but not with RT97⁺ fibers. These results suggest that the sprouting of unmyelinated nociceptive pelvic afferents following high thoracic SCI, but not myelinated fibers, contributes to hypertensive autonomic dysreflexia induced by pelvic visceral pain.

Indexing terms

distal colon; cholera toxin subunit beta; pelvic primary afferent; neuronal plasticity

INTRODUCTION

Autonomic dysreflexia is a potentially life-threatening hypertensive syndrome that develops after spinal cord injury (SCI) above the sixth thoracic (T) spinal segment. It is characterized by severe hypertension due to sudden, massive discharge of the sympathetic preganglionic neurons below the injury site, which when accompanied by baroreflex-mediated bradycardia defines this syndrome (Finestone and Teasell, 1993; Zagon and Smith, 1993). Autonomic dysreflexia is commonly triggered by noxious stimuli below the injury site, particularly by the distension of pelvic viscera (bowel and bladder) (Lindan et al., 1980; Karlsson, 1999). It is believed that acute autonomic dysreflexia arises due to loss of bulbospinal sympathetic

^{*}Corresponding Author: Alexander G. Rabchevsky, Ph.D., Associate Professor of Physiology, University of Kentucky, Spinal Cord & Brain Injury Research Center (SCoBIRC), B471, Biomedical & Biological Sciences Research Building, 741 South Limestone Street, Lexington, KY 40536-0509, Office: (859) 323-0267, Fax: (859) 257-5737, AGRab@uky.edu.

[#]Authors contributed equally

inhibition (Krassioukov and Weaver, 1995, 1996). This is followed by injury-induced increases in growth factor expression (Brown et al., 2004) that elicit progressive structural and electrophysiological changes in both primary afferents and spinal neurons that coincide with increased severity of autonomic dysreflexia (Maiorov et al., 1997; Weaver et al., 1997; Krenz and Weaver, 1998b, a; Chau et al., 2000). Moreover, studies from our lab have shown that following complete T4 spinal transection, both primary afferent fiber sprouting into lumbosacral (L/S) dorsal horns (Cameron et al., 2006) and plasticity of L/S propriospinal neurons in the dorsal gray commissure (DGC) (Hou et al., 2008) correlate temporally with the development of autonomic dysreflexia.

Nevertheless, there is still uncertainty regarding which branch of the pelvic primary afferents, the myelinated or unmyelinated fibers, contribute to the development of autonomic dysreflexia. The unmyelinated pelvic afferent fibers, which convey thermal and nociceptive information, have been shown to contain calcitonin gene-related peptide (CGRP) (Keast and De Groat, 1992). Alternatively, the monoclonal antibody for 200 kDa neurofilament subunit in phosphorylated form, RT97, which is exclusively expressed in A-fiber afferent neurons, is a marker for myelinated primary afferent fibers in both somatic and visceral nerves (Perry et al., 1991; Sann et al., 1995; Wang et al., 1998). Yoshimura et al (1998) reported that capsaicin-sensitive neurons (unmyelinated fibers) in L6/S1 dorsal root ganglia (DRG) were dramatically reduced in spinal transected rats compared to shams. Conversely, neurofilament-rich DRG neurons (myelinated fibers) were detected at a significantly greater percentage after spinal cord transection (Yoshimura et al., 1998). On the contrary, we and others have shown that experimental autonomic dysreflexia induced by noxious colorectal distension (CRD) in spinal transected rats correlates with profuse nerve growth factor (NGF)-mediated intraspinal sprouting of CGRP⁺ primary afferent fibers into L/S spinal segments (termination sites of pelvic visceral sensory axons) (Krenz and Weaver, 1998a; Weaver et al., 2001; Cameron et al., 2006; Rabchevsky, 2006).

Primary sensory afferent fibers innervating the descending colon in rats run in the pelvic and hypogastric/lumbar colonic nerves, distributing mainly to the L6/S1 spinal level (Ness and Gebhart, 1987; Al-Chaer and Traub, 2002). To characterize the relative contribution of myelinated versus unmyelinated sensory fiber sprouting to the development of autonomic dysreflexia, cholera toxin subunit beta (CTb) was injected into the distal colon of selected T4-transected versus sham rats to label distal colonic afferents and their terminal arbors within the L/S spinal cord. Our results demonstrate, for the first time, that following high thoracic SCI, the sprouting of unmyelinated nociceptive pelvic afferents into the L/S spinal cord, but not myelinated fibers, is correlated with dysreflexic hypertension induced by visceral pain.

EXPERIMENTAL PROCEDURES

Animals and surgery

All animal housing conditions, surgical procedures and post-operative care techniques were conducted according to the University of Kentucky Institutional Animal Care and Use Committee and the National Institutes of Health animal care guidelines. Adult female Wistar rats (~200–250g) were anesthetized with a mixture of ketamine (80 mg/kg, i.p.; Fort Dodge Animal Health, Fort Dodge, IA) and xylazine (10 mg/kg, i.p.; Butler, Columbus, OH). The injured group received complete T4 transection following T3 vertebral laminectomy (n=18), in contrast to the sham group which received only T3 laminectomy (n=15).

The spinal cord was completely transected with a #11 scalpel blade at the T4 level following the laminectomy, as described previously (Cameron et al., 2006). After surgical operations were complete, the erector spinae muscles were sutured with 3-0 Vycril (Ethicon,

Sommerfield, NJ), the field was disinfected with povidone-iodine solution (Nova Plus, Irving, TX), and the skin was closed with Michel wound clips (Roboz, Gaithersburg, MD). For post-operative care, animals were administered 20 ml lactated Ringer's solution (Baxter Healthcare, Deerfield, IL) and 33 mg/kg cephazolin (Apothecon, Bristol-Myers Squibb, Princeton, NJ) subcutaneously immediately after surgery, and for injured rats twice daily for up to 10 days to maintain hydration and control infection. Buprenorphine (0.035 mg/kg; Reckitt Benckiser, UK) was also administered subcutaneously once after recovery from anesthesia and twice daily for the next three days to control post-operative pain. Bladders of injured rats were manually expressed twice daily until automatic bladder-emptying reflex developed at about 10 days post injury.

CTb injections and tracing

Two weeks after injury/sham, selected T4-transected (n=7) and non-transected (n=7) rats were reanesthetized with ketamine (80 mg/kg, i.p.) and xylazine (10 mg/kg, i.p.) to inject the distal colon with CTb, as previously described with modifications (Valentino et al., 2000). Briefly, a laparotomy was made to expose the pelvic viscera. With a Hamilton microsyringe (33-gauge needle; Hamilton, Reno, NV), 6 μ l of CTb solution (1% in dH₂O; List Biological Laboratories, Campbell, CA) was injected circumferentially beneath the serosal layer in the distal colon, 1–2 cm proximal to the anus. The injections were made in 6 adjacent sites surrounding the colon (1 μ l/site). Injection sites were sealed with a drop of tissue adhesive (3M Vetbond™, St. Paul, MN, USA) to minimize leakage of tracer before the wound was sutured. To control for CTb labeling specificity, CTb solution was topically applied on the ventral surface of the distal colon of an additional sham and an injured rat (n=1 per group). After 1 week post-CTb injection to allow for transport, animals were perfused and spinal cords were harvested for histology.

Assessing autonomic dysreflexia with colorectal distension

Two weeks after T4 spinal transection, femoral cannulas were implanted in 3 randomly selected rats to verify the incidence of autonomic dysreflexia during noxious colorectal distension (CRD) the following day, as detailed previously (Cameron et al., 2006). An injured rat was regarded as dysreflexic if CRD, produced by inflation of a cardiac catheter balloon at a pressure that is known to stimulate the nociceptive fibers, created a rise in mean arterial pressure (MAP) and a concomitant decrease in heart rate (HR) for as long as the period of CRD.

Dissection and tissue processing

Three weeks after T4-transection/sham (n=33), including 1 week post-CTb injections in the tracing cohort (n=7 per group), animals were overdosed with sodium pentobarbital (150 mg/kg; Abbott, Chicago, IL) and perfused transcardially with 0.1 M phosphate buffered saline (PBS), pH 7.4, followed by 4% paraformaldehyde in PBS. A 6 cm long spinal cord extending from the conus medullaris to the transection site was removed, post-fixed for 4 hours, rinsed in 0.2 M phosphate buffer (PB) overnight, and cryoprotected in 20% sucrose in 0.1 M PBS. The 3 cm caudal segments (~T12-S3) were embedded in gum tragacanth (Sigma-Aldrich, St. Louis, MO) in 20% sucrose/PBS for cryosectioning, as previously detailed (Cameron et al., 2006). Embedded spinal cord segments were snap-frozen in acetone chilled to -40°C and stored at -80°C until sectioning on a cryostat (Microm Laborgerate, Walldorf, Germany). Approximately 30 consecutive rows of 20 μ m transverse cryosections separated by 100 μ m from each spinal cord were placed onto each of 10 adjacent glass slides (Superfrost plus, Fisher Scientific, Pittsburgh, PA) in two series, as previously detailed (Cameron et al., 2006). All mounted slides were stored at -20°C until staining procedures.

Immunofluorescent histochemistry

The complete information of all primary antibodies used is detailed in Table 1. For CTb staining, slides with mounted coronal sections were thawed and pre-incubated in 0.1 M PBS containing 0.5% Triton-X and 5% normal donkey serum (Vector Laboratories, Burlingame, CA) for 1 hour, followed by incubation with goat anti-CTb (List Biological Laboratories, Campbell, CA, 1:1500) in same buffer overnight at 4°C. The slides were then rinsed before applying donkey anti-goat conjugated to FITC (Jackson ImmunoResearch Laboratories, West Grove, PA; 7.5µg/ml) for 3 hours at room temperature.

For CGRP⁺ or RT97⁺ afferent fibers, immunohistochemical staining was conducted with rabbit anti-rat CGRP (Sigma-Aldrich, Saint Louis, MI, 1:2000) or mouse anti-rat RT97 (Chemicon, Temecula, CA, 0.25µg/ml) on coronal sections. Sections were pre-incubated in 0.1 M PBS containing 0.5% Triton-X and 5% normal donkey serum for 1 hour at room temperature, followed by incubation with primary antibodies in the same buffer overnight at 4°C. The slides were then rinsed before applying secondary antibodies for 3 hours at room temperature. The secondary antibodies were donkey anti-rabbit or donkey anti-mouse conjugated to Texas-Red (Jackson ImmunoResearch Laboratories, West Grove, PA; 7.5µg/ml). To observe whether CTb-labeled afferents co-localized with either CGRP⁺ or RT97⁺ fiber, double immunostaining with both CTb and CGRP or RT97 antibodies was conducted. In addition, double immunostaining for both CGRP and RT97 antibodies was performed to rule out possible co-localization.

Using commercially available monoclonal or polyclonal antibodies against rat choline acetyltransferase (ChAT), we were unable to successfully double-label ChAT in putative autonomic or somatic motoneurons with the CTb antibody we employed. Therefore, the remaining series of sections were incubated with reliable goat anti-human ChAT (Chemicon, Temecula, CA, 1:100) overnight at 4°C, followed by donkey anti-goat conjugated to Texas Red (Jackson ImmunoResearch Laboratories, West Grove, PA; 7.5µg/ml) for 3 hours at room temperature.

All control slides had the primary antibody omitted before applying the secondary. After final rinses, slides were coverslipped using Vectashield mounting medium (Vector, Burlingame, CA) containing 5 µM Hoechst 33342 nuclear dye (Sigma-Aldrich, Saint Louis, MI), and sealed with Cutex nail hardener (Jackson, WY). Adobe Photoshop 7.0 was used to manipulate photomicrographs only for brightness/contrast and to construct all figures.

CTb-labeling and densitometric quantification

An Olympus IX81 spinning confocal microscope (Olympus Corp. Melville, NY) was used for high magnification dual immunofluorescence microscopy of CTb-labeled cells. For all densitometric analyses, including RT97⁺ myelinated and CGRP⁺ unmyelinated fibers, digital images were captured using an Optronics digital video camera (Optronics Corp., Goleta, CA). Densitometry for both groups, with and without CTb tracing, was conducted in a blinded fashion using the Bioquant[®] image analysis program (Nova Prime, V6.70.10; Bioquant Image Analysis Corp., Nashville, TN) on coronal sections viewed under an Olympus BX51 microscope (Olympus Corp. Melville, NY) using established methods (Cameron et al., 2006; Rabchevsky et al., 2007).

All sections were photographed with the same 10x objective magnification (10x eye piece) and with the same exposure settings. In all sections analyzed, our region of interest encompassed the unilateral (right) dorsal gray matter above the central canal, including Lissauer's tract (LT) on the surface of dorsal horn (Fig. 1). Since CTb-labeled cells were seen in the sacral parasympathetic nucleus (SPN), this region was excluded from all densitometric analyses (see Discussion, Methodological considerations). For each animal,

three serial spinal cord sections separated by 1 mm and centering on the L6/S1 level, as identified by cytoarchitecture, were selected for quantification. To measure CTb⁺/CGRP⁺/RT97⁺ immunoreactivity, labeled fibers were “thresholded” on each digital photograph, using the Bioquant program. For each section, the percent area occupied by immunolabeled fibers was calculated as the ratio of immunoreactive area divided by the region of interest area in unilateral dorsal gray matter x 100. The mean percentage of immunoreactive area occupied in three sections was calculated, followed by the mean for all animals in a treatment group.

Statistical analysis

Unpaired Student's t-tests were used to compare data between T4-transected and non-transected groups, using StatView (SAS Institute, Cary, NC). Significance throughout all experiments was set at $P < 0.05$. Data are represented as mean \pm SD.

RESULTS

Autonomic dysreflexia: noxious CRD-induced changes in MAP and HR

In all three selected rats with T4-transection, CRD performed 2 weeks post-SCI elicited MAP increases accompanied by reduced HR characteristic of autonomic dysreflexia (data not shown). These results are in accordance with what we have published (Cameron et al., 2006).

Sprouting of pelvic primary afferents without CTb tracing

Unmyelinated CGRP⁺ afferents—In both T4-transected and sham rats, CGRP immunoreactivity was predominately expressed in fibers and punctate terminals in three regions: the superficial dorsal horn (laminae I–II), medial gray matter (above the central canal), as well as peri-sacral parasympathetic nucleus (SPN) throughout the lumbosacral spinal cord (Fig. 2). Lissauer's tract located above lamina I and along the lateral edge of the dorsal horn were also immunolabeled (Nadelhaft and Booth, 1984). In addition, CGRP⁺ branching fibers in laminae III–V extended individually and in bundles towards the dorsal gray commissure (DGC; lamina X). Notably, CGRP⁺ fibers could not be seen extending into the ventral horn in either T4-transected or sham spinal cords (Fig. 2A–D). However, CGRP⁺ neurons were frequently observed in the ventral horn of both groups (Fig. 2A).

Qualitatively, CGRP labeling density and distribution in laminae I–II at the L6/S1 level appeared similar in T4-transected and sham rats. However, following injury the density of CGRP⁺ fibers appeared increased in other regions, particularly in laminae III–V and DGC (Fig. 2A–D). Statistical analysis demonstrated that the density of CGRP⁺ fibers in the dorsal horns was significantly ($P < 0.05$) greater in L6/S1 gray matter of T4-transected spinal cords compared to shams (Fig. 2E).

Myelinated RT97⁺ afferents—Throughout the lumbosacral segments, RT97⁺ fibers in the gray matter could be observed from dorsal to ventral in both T4-transected and non-transected spinal cords (Fig. 3). The most intense immunoreactivity was located in laminae III–VI, where bundles of RT97⁺ fibers could be seen to extend towards the medial gray matter in coronal sections. Conversely, very few positive fibers were observed in laminae I–II. The distribution and density of RT97⁺ fibers appeared similar in T4-transected versus sham rats (Fig. 3A, B), and statistical analysis confirmed this observation ($P > 0.1$) (Fig. 3C).

CTb-labeling of unmyelinated versus myelinated pelvic primary afferents

CTb tracing—One week after CTb injections into the distal colon, CTb-labeled fibers could be detected in lumbosacral segments in both sham and T4-transected spinal cords. The immunoreactivity was predominantly observed at the L6/S1 levels, bilaterally. CTb-labeled central projections of colonic primary afferent were exclusively distributed within Lissauer's tract, laminae I–II, medial gray matter (DGC), as well as the vicinity of the SPN (Fig. 4A), similar to the CGRP labeling pattern described above. CTb-labeled collateral fibers from Lissauer's tract entered the gray matter via two pathways; a prominent lateral collateral projection (LCP) and a much less prominent medial collateral projection (MCP) (Nadelhaft and Booth, 1984), which formed a thin layer in the marginal zone surrounding the dorsal horn (Fig. 4B, C). CTb-labeled LCP separated into two branches (lateral and medial) in the dorsolateral funiculus close to the lateral border of the dorsal horn and entered the intermediate gray matter. The lateral branch entered the region of the SPN and intermingled with neurons, whereas the medial branch extended into the DGC, often with labeled fibers crossing the midline. CTb-labeled fibers within the MCP were located along the dorsomedial border of the dorsal horn and extended into the DGC. In most instances, CTb-labeled afferents in T4-transected spinal cords appeared greater than shams (Fig. 5A, B). Statistical analysis showed that the density of CTb-labeled colonic afferents in the L6/S1 spinal level was significantly ($P < 0.05$) increased after T4-transection (Fig. 5C).

Notably, labeling was observed in both T4-transected and sham cords. At the L1/L2 spinal level, CTb-labeled cell clusters were observed in the DGC and to a lesser extent in the intermediolateral cell column (IML) (Fig. 6A, C). Positive immunostaining for ChAT in an adjacent slide series revealed that these CTb-labeled cells are likely a sub-population of sympathetic preganglionic neurons (Fig. 7A, C). At the L6/S1 spinal level, CTb-labeled cell clusters were prominent in the SPN, bilaterally (Fig. 6B, E). Positive immunostaining for ChAT in an adjacent slide series indicated that these cells were cholinergic, parasympathetic preganglionic neurons (Fig. 7B, E). Processes from these neurons formed a pattern extending deep into the dorsolateral funiculus to the border of the spinal cord (see Figs. 4 and 5). Many of these fibers extended medially into the DGC and across the midline, a typical dendritic pattern of autonomic preganglionic neurons (Hosoya et al., 1994). Since these processes were negative for CGRP, hence not primary afferent fibers, they were excluded from quantification of CTb-labeled fiber density.

Throughout the lumbosacral spinal cord, putative somatic motoneurons with large-diameter cell bodies and stout extensions in the ventral horn were also labeled (Fig. 6B, D). Positive immunostaining for ChAT in an adjacent slide series indicated that these CTb-labeled cells were cholinergic motoneurons (Fig. 7B, D). The frequency and distribution of CTb-labeled motoneurons however, was highly variable, even within injury/sham cohorts. After we quantified all CTb-labeled motoneurons in 6 serial slide series (~T12–S3) from both sham ($n=3$) and transected ($n=3$) spinal cords (144 sections per animal, each separated by 100 μm), we found 0–3 labeled cells in each section, bilaterally. This corresponded to a sum of 50 labeled motoneurons in thoracolumbar segments (~T12–L2) and 98 motoneurons in the lumbosacral segments (~L3–S3) of all spinal cords examined. As injury did not appear to alter these numbers, the lumbosacral segments had a two-fold increase in the number of CTb-labeled motoneurons.

To verify the possibility of tracer leakage resulting in the labeling of autonomic preganglionic neurons, 6 μl of CTb tracer was sprayed over the surface of the distal colon in designated rats. After 1 week, however, we did not observe any labeled autonomic preganglionic neurons, primary central projections, or motoneurons in the lumbosacral spinal cord of both sham and injured groups.

Sprouting of unmyelinated and myelinated pelvic afferents with CTb tracing—

CTb-labeled lumbosacral spinal cords were immunostained for unmyelinated (CGRP⁺) and myelinated (RT97⁺) primary sensory afferents, respectively. The distribution patterns within the gray matter appeared similar to the group without CTb tracing (see Figs. 2 and 3). Statistical analysis confirmed significantly ($P < 0.05$) greater CGRP⁺ fiber density in T4-transected spinal cords versus shams, whereas no significant ($P > 0.1$) change was detected in RT97⁺ fiber density at the L6/S1 spinal level following injury (Fig. 8).

Phenotypic characterization of CTb-labeled fibers—Double immunostaining demonstrated that CTb-labeled colonic primary afferent fibers were co-localized with CGRP⁺ afferent fibers (Fig. 9A–F). On the contrary, no co-localization was observed between CTb-labeled pelvic afferents and RT97⁺ fibers (Fig. 9G–I). Furthermore, there was no co-localization between RT97⁺ and CGRP⁺ fibers in the lumbosacral spinal segments (data not shown).

DISCUSSION

Utilizing neuronal tract tracing and immunohistochemical methods, the major finding in the present study is that only unmyelinated pelvic visceral afferent fiber sprouting occurs in the lumbosacral level following high thoracic spinal cord transection. In addition, following CTb injections into the distal colon, the density of labeled colonic afferents at the L6/S1 spinal level was significantly enhanced at 3 weeks post-injury compared to sham spinal cords. Furthermore, virtually all CTb-labeled colonic afferent fibers in the lumbosacral spinal cord co-localized with CGRP⁺ unmyelinated fibers.

CTb tracing

To date, CTb has been used to trace and characterize colonic afferent phenotypes only in the dorsal root ganglion of normal mice, which demonstrated that the majority are unmyelinated (Christianson et al., 2006). This is supported by studies in normal rats where CTb is retrogradely transported mainly by unmyelinated fibers in bladder afferents, in contrast to somatic nerves that are primarily myelinated (Wang et al., 1998). However, there have been no reports on the sprouting of CTb-labeled colonic afferents in spinalized versus normal rats, which is critical to establish since our model employs noxious colorectal distension to elicit autonomic dysreflexia. In somatic primary afferents, CTb has been used to identify thinly myelinated DRG neurons/processes through its binding to the ganglioside (GM1) receptor (Robertson and Grant, 1985, 1989; LaMotte et al., 1991; Robertson et al., 1991; Krenz and Weaver, 1998b). It has been reported that CTb injections into quadriceps muscles labeled central arbors of somatic, presumptive myelinated primary afferents via the sciatic nerve (Krenz and Weaver, 1998b). However, unlike somatic nerves, visceral nerves do not contain many large diameter myelinated fibers but are composed of unmyelinated C-fibers and thinly myelinated A δ -fibers (Sengupta and Gebhart, 1994). Colonic afferents are largely composed of unmyelinated C-fibers and a relatively low percentage of myelinated A δ -fibers (Christianson et al., 2006). Following injection into urinary bladder wall, CTb conjugated to horseradish peroxidase (HRP) has been reported to be predominantly transported by unmyelinated fibers in visceral afferent fibers (Wang et al., 1998). Importantly, following our distal colon injections all CTb-labeled colonic afferents co-localized with CGRP⁺ but not RT97⁺ fibers. This indicates the preferential uptake of CTb by unmyelinated versus myelinated fibers, specifically in pelvic primary afferent fibers.

In the rat, primary sensory information from the distal colon is conveyed via the pelvic and hypogastric nerves (Al-Chaer and Traub, 2002; Christianson et al., 2006). The visceral primary afferents from the pelvic nerve enter the spinal cord through Lissauer's tract and

lamina I, projecting to the SPN via the LCP and to the DGC region via the LCP and MCP (Morgan et al., 1981; Nadelhaft and Booth, 1984). Our CTb⁺ colonic afferent fiber labeling results are consistent with these reports. While the increase in CTb-labeled fiber density is consistent with sprouting of CGRP⁺ pelvic afferents, there are certain caveats and methodological issues that should be considered.

Methodological considerations

In preliminary studies we found that CTb-labeled afferent fibers were mainly distributed within L1-L2 spinal level after tracer injection into the mid-distal colon. This is likely because primary afferent fibers from the mid-distal colon enter the L1-L2 spinal cord through hypogastric/lumbar colonic nerve, but primary afferents in the caudal part of distal colon innervate the L6/S1 spinal cord via the pelvic nerve (Ness and Gebhart, 1987; Al-Chaer and Traub, 2002). Since autonomic dysreflexia is normally triggered by noxious pelvic stimuli, which is relayed via the pelvic nerve to the spinal cord, we injected CTb in sub-serosal layers proximal to the rectum to ensure consistent labeling of the pelvic nerve.

In the present study we observed CTb-labeled somatic motoneurons and their dendrites in the lumbosacral ventral horns. Although we had controls for tracer leakage, this labeling could possibly be explained by tracer diffusion into sphincter muscles during sub-serosal injections, which is subsequently transported to the spinal cord via the pudendal nerve. The distribution, size and morphology of these motoneurons are in accordance with retrograde tracing studies of the pudendal nerve with horseradish peroxidase (HRP) and other tracers injected into perineal muscles (McKenna and Nadelhaft, 1986). In particular, anal sphincter motoneurons were localized in the ventral-most aspects of ventral horns, similar to what we observed.

Sympathetic preganglionic neurons at the L1/L2 spinal level and SPN neurons at the L6/S1 spinal level were also labeled by CTb injections into the distal colon. These results are comparable with those following direct injection of HRP into the hypogastric and pelvic nerves (Hancock and Peveto, 1979; Nadelhaft and Booth, 1984). One possibility is tracer leakage and uptake by autonomic preganglionic neurons. However, topical application CTb solution on the ventral surface of distal colon did not label either sympathetic or parasympathetic preganglionic neurons. Alternatively, cells could be labeled through the uptake of CTb by pelvic efferent fibers en passage (Chen and Aston-Jones, 1995; Chen et al., 1999). Another possibility is that CTb might have been injected inadvertently into the inferior mesenteric or pelvic ganglia, due to their close proximity to the wall of the distal colon. Thus, the specific means by which CTb is transported to autonomic preganglionic neurons and motoneurons following injections into the colorectum likely stems from perturbation of their respective nerve endings at the multiple injection sites.

Sprouting of pelvic primary afferents after SCI

In somatic nerves, myelinated primary afferent fibers convey sensations of touch, vibration and limb position (A β -fiber), and higher-threshold stimulation (A δ -fiber). The central arbors of large diameter myelinated A β primary afferent fibers predominantly terminate in laminae III–V of the dorsal horn, as well as in Clarke's nucleus (LaMotte et al., 1991; Rivero-Melian and Grant, 1991; Wilson and Kitchener, 1996). The small diameter A δ myelinated fibers arborize mostly in lamina I (Rivero-Melian et al., 1992; Wilson and Kitchener, 1996). Unlike their somatic counterparts, visceral nerves are composed of unmyelinated C-fibers and thinly myelinated A δ -fibers (Vera and Nadelhaft, 1990). Unmyelinated afferent fibers primarily terminate in laminae I, II and V, lamina X above the central canal (DGC) (Hancock and Peveto, 1979; Hosoya et al., 1994), as well as the lateral gray matter (Pascual et al., 1993; Matsushita, 1998; Vizzard, 2000). Previously, it was shown that although the

number of CGRP⁺ DRG neurons remained unchanged after SCI, CGRP⁺ afferent fiber density in the dorsal horns and lateral gray matter increased at the lumbosacral spinal levels (L1-S1) (Krenz and Weaver, 1998b). The present study further confirms the sprouting of unmyelinated pelvic visceral afferents in the lumbosacral spinal cord following high thoracic SCI.

CGRP⁺ DRG neurons express the high-affinity Trk A receptor (Averill et al., 1995), and increases in NGF levels after SCI could induce the sprouting of unmyelinated primary sensory neurons. Indeed, using adenovirus encoding NGF (Cameron et al., 2006), we have shown that a contributing factor to the severity of CRD-induced dysreflexic hypertension is elevation in NGF-responsive CGRP⁺ nociceptive sensory afferents at L6/S1 spinal level, similar to previous reports (Krenz and Weaver, 1998b; Weaver et al., 2001). Consequently, elevated intraspinal NGF after SCI is one of main triggers for the sprouting of CGRP⁺ unmyelinated pelvic visceral afferents in the lumbosacral spinal cord. Along with our recent finding of lumbosacral propriospinal plasticity following high thoracic SCI (Hou et al., 2008), the sprouting of unmyelinated CGRP⁺ pelvic primary afferents in lumbosacral spinal cord could facilitate enhanced transmission of nociceptive pelvic stimuli to thoracolumbar sympathetic preganglionic neurons in episodic hypertension. Interestingly, the use of CGRP receptor antagonists was found to block the development of dorsal horn neuron hyperexcitability in response to peripheral inflammation (Neugebauer et al., 1996). Moreover, a subpopulation of CGRP⁺ fiber sprouts below an injury site have been suggested to be anatomical substrates for chronic pain syndromes (Christensen and Hulsebosch, 1997; Ondarza et al., 2003).

CONCLUSION

In summary, the present study demonstrates that following high thoracic SCI the selective sprouting of CGRP⁺ unmyelinated nociceptive pelvic afferents into the lumbosacral spinal cord correlates with the development of autonomic dysreflexia. Furthermore, CTb injections into the distal colon predominately labeled unmyelinated pelvic visceral afferent fibers, in contrast to previous studies in which myelinated somatic afferent fibers were labeled with CTb. Our results demonstrate that the sprouting of unmyelinated nociceptive pelvic afferents, but not myelinated fibers, likely mediates the initiation of CRD-evoked autonomic dysreflexia. Future studies will focus on employing viral-mediated site-specific over-expression of neurotrophin-3 (NT-3) to enhance the survival and growth of myelinated mechanoreceptive and/or proprioceptive sensory neurons to rule out the contribution of myelinated fiber sprouting to the development of autonomic dysreflexia.

Acknowledgments

This work was supported by grants from KSCHIRT #3-11 (AGR), NIH/NINDS R01 NS049901-01 (AGR) and P30 NS051220. Authors are grateful for the technical expertise of Travis Lyttle, M.S. and Joseph Whelan, M.S..

Abbreviations

SCI	spinal cord injury
T	thoracic
L/S	lumbosacral
CTb	cholera toxin subunit beta
CGRP	calcitonin gene-related peptide

ChAT	choline acetyltransferase
DGC	dorsal gray commissure
SPN	sacral parasympathetic nucleus
CRD	colorectal distension
NGF	nerve growth factor
DRG	dorsal root ganglia
HR	heart rate
MAP	mean arterial pressure
FB	fast blue
LCP	lateral collateral projection
MCP	medial collateral projection
NT-3	neurotrophin-3

References

- Al-Chaer ED, Traub RJ. Biological basis of visceral pain: recent developments. *Pain*. 2002; 96:221–225. [PubMed: 11972993]
- Averill S, McMahon SB, Clary DO, Reichardt LF, Priestley JV. Immunocytochemical localization of trkA receptors in chemically identified subgroups of adult rat sensory neurons. *Eur J Neurosci*. 1995; 7:1484–1494. [PubMed: 7551174]
- Brown A, Ricci MJ, Weaver LC. NGF message and protein distribution in the injured rat spinal cord. *Exp Neurol*. 2004; 188:115–127. [PubMed: 15191808]
- Cameron AA, Smith GM, Randall DC, Brown DR, Rabchevsky AG. Genetic manipulation of intraspinal plasticity after spinal cord injury alters the severity of autonomic dysreflexia. *J Neurosci*. 2006; 26:2923–2932. [PubMed: 16540569]
- Chau D, Johns DG, Schramm LP. Ongoing and stimulus-evoked activity of sympathetically correlated neurons in the intermediate zone and dorsal horn of acutely spinalized rats. *J Neurophysiol*. 2000; 83:2699–2707. [PubMed: 10805670]
- Chen S, Aston-Jones G. Evidence that cholera toxin B subunit (CTb) can be avidly taken up and transported by fibers of passage. *Brain Res*. 1995; 674:107–111. [PubMed: 7773677]
- Chen S, Yang M, Miselis RR, Aston-Jones G. Characterization of transsynaptic tracing with central application of pseudorabies virus. *Brain Res*. 1999; 838:171–183. [PubMed: 10446330]
- Christensen MD, Hulsebosch CE. Chronic central pain after spinal cord injury. *J Neurotrauma*. 1997; 14:517–537. [PubMed: 9300563]
- Christianson JA, Traub RJ, Davis BM. Differences in spinal distribution and neurochemical phenotype of colonic afferents in mouse and rat. *J Comp Neurol*. 2006; 494:246–259. [PubMed: 16320237]
- Finestone HM, Teasell RW. Autonomic dysreflexia after brainstem tumor resection. A case report. *Am J Phys Med Rehabil*. 1993; 72:395–397. [PubMed: 8260135]
- Hancock MB, Peveto CA. Preganglionic neurons in the sacral spinal cord of the rat: an HRP study. *Neurosci Lett*. 1979; 11:1–5. [PubMed: 86176]
- Hosoya Y, Nadelhaft I, Wang D, Kohno K. Thoracolumbar sympathetic preganglionic neurons in the dorsal commissural nucleus of the male rat: an immunohistochemical study using retrograde labeling of cholera toxin subunit B. *Exp Brain Res*. 1994; 98:21–30. [PubMed: 8013588]
- Hou S, Duale H, Cameron AA, Abshire SM, Lyttle TS, Rabchevsky AG. Plasticity of lumbosacral propriospinal neurons is associated with the development of autonomic dysreflexia after thoracic spinal cord transection. *J Comp Neurol*. 2008; 509:382–399. [PubMed: 18512692]
- Karlsson AK. Autonomic dysreflexia. *Spinal Cord*. 1999; 37:383–391. [PubMed: 10432257]

- Keast JR, De Groat WC. Segmental distribution and peptide content of primary afferent neurons innervating the urogenital organs and colon of male rats. *J Comp Neurol.* 1992; 319:615–623. [PubMed: 1619047]
- Krassioukov AV, Weaver LC. Episodic hypertension due to autonomic dysreflexia in acute and chronic spinal cord-injured rats. *Am J Physiol.* 1995; 268:H2077–2083. [PubMed: 7771558]
- Krassioukov AV, Weaver LC. Morphological changes in sympathetic preganglionic neurons after spinal cord injury in rats. *Neuroscience.* 1996; 70:211–225. [PubMed: 8848126]
- Krenz NR, Weaver LC. Changes in the morphology of sympathetic preganglionic neurons parallel the development of autonomic dysreflexia after spinal cord injury in rats. *Neurosci Lett.* 1998a; 243:61–64. [PubMed: 9535113]
- Krenz NR, Weaver LC. Sprouting of primary afferent fibers after spinal cord transection in the rat. *Neuroscience.* 1998b; 85:443–458. [PubMed: 9622243]
- LaMotte CC, Kapadia SE, Shapiro CM. Central projections of the sciatic, saphenous, median, and ulnar nerves of the rat demonstrated by transganglionic transport of cholera toxin B-subunit (B-HRP) and wheat germ agglutinin-HRP (WGA-HRP). *J Comp Neurol.* 1991; 311:546–562. [PubMed: 1721924]
- Lindan R, Joiner E, Freehafer AA, Hazel C. Incidence and clinical features of autonomic dysreflexia in patients with spinal cord injury. *Paraplegia.* 1980; 18:285–292. [PubMed: 7443280]
- Maiorov DN, Krenz NR, Krassioukov AV, Weaver LC. Role of spinal NMDA and AMPA receptors in episodic hypertension in conscious spinal rats. *Am J Physiol.* 1997; 273:H1266–1274. [PubMed: 9321815]
- Matsushita M. Ascending propriospinal afferents to area X (substantia grisea centralis) of the spinal cord in the rat. *Exp Brain Res.* 1998; 119:356–366. [PubMed: 9551836]
- McKenna KE, Nadelhaft I. The organization of the pudendal nerve in the male and female rat. *J Comp Neurol.* 1986; 248:532–549. [PubMed: 3722467]
- Morgan C, Nadelhaft I, de Groat WC. The distribution of visceral primary afferents from the pelvic nerve to Lissauer's tract and the spinal gray matter and its relationship to the sacral parasympathetic nucleus. *J Comp Neurol.* 1981; 201:415–440. [PubMed: 7276258]
- Nadelhaft I, Booth AM. The location and morphology of preganglionic neurons and the distribution of visceral afferents from the rat pelvic nerve: a horseradish peroxidase study. *J Comp Neurol.* 1984; 226:238–245. [PubMed: 6736301]
- Ness TJ, Gebhart GF. Characterization of neuronal responses to noxious visceral and somatic stimuli in the medial lumbosacral spinal cord of the rat. *J Neurophysiol.* 1987; 57:1867–1892. [PubMed: 3598634]
- Neugebauer V, Rumenapp P, Schaible HG. Calcitonin gene-related peptide is involved in the spinal processing of mechanosensory input from the rat's knee joint and in the generation and maintenance of hyperexcitability of dorsal horn-neurons during development of acute inflammation. *Neuroscience.* 1996; 71:1095–1109. [PubMed: 8684614]
- Ondarza AB, Ye Z, Hulsebosch CE. Direct evidence of primary afferent sprouting in distant segments following spinal cord injury in the rat: colocalization of GAP-43 and CGRP. *Exp Neurol.* 2003; 184:373–380. [PubMed: 14637107]
- Pascual JI, Insausti R, Gonzalo LM. Urinary bladder innervation in male rat: termination of primary afferents in the spinal cord as determined by transganglionic transport of WGA-HRP. *J Urol.* 1993; 150:500–504. [PubMed: 7686986]
- Perry MJ, Lawson SN, Robertson J. Neurofilament immunoreactivity in populations of rat primary afferent neurons: a quantitative study of phosphorylated and non-phosphorylated subunits. *J Neurocytol.* 1991; 20:746–758. [PubMed: 1960537]
- Rabchevsky AG. Segmental organization of spinal reflexes mediating autonomic dysreflexia after spinal cord injury. *Prog Brain Res.* 2006; 152:265–274. [PubMed: 16198706]
- Rabchevsky AG, Sullivan PG, Scheff SW. Temporal-spatial dynamics in oligodendrocyte and glial progenitor cell numbers throughout ventrolateral white matter following contusion spinal cord injury. *Glia.* 2007; 55:831–843. [PubMed: 17390308]

- Rivero-Melian C, Grant G. Choleragenoid horseradish peroxidase used for studying projections of some hindlimb cutaneous nerves and plantar foot afferents to the dorsal horn and Clarke's column in the rat. *Exp Brain Res.* 1991; 84:125–132. [PubMed: 1713167]
- Rivero-Melian C, Rosario C, Grant G. Demonstration of transganglionically transported choleragenoid in rat spinal cord by immunofluorescence cytochemistry. *Neurosci Lett.* 1992; 145:114–117. [PubMed: 1281298]
- Robertson B, Grant G. A comparison between wheat germ agglutinin-and choleragenoid-horseradish peroxidase as anterogradely transported markers in central branches of primary sensory neurones in the rat with some observations in the cat. *Neuroscience.* 1985; 14:895–905. [PubMed: 3838806]
- Robertson B, Grant G. Immunocytochemical evidence for the localization of the GM1 ganglioside in carbonic anhydrase-containing and RT 97-immunoreactive rat primary sensory neurons. *J Neurocytol.* 1989; 18:77–86. [PubMed: 2496205]
- Robertson B, Perry MJ, Lawson SN. Populations of rat spinal primary afferent neurons with choleragenoid binding compared with those labelled by markers for neurofilament and carbohydrate groups: a quantitative immunocytochemical study. *J Neurocytol.* 1991; 20:387–395. [PubMed: 1869879]
- Sann H, McCarthy PW, Jancso G, Pierau FK. RT97: a marker for capsaicin-insensitive sensory endings in the rat skin. *Cell Tissue Res.* 1995; 282:155–161. [PubMed: 8581918]
- Sengupta JN, Gebhart GF. Characterization of mechanosensitive pelvic nerve afferent fibers innervating the colon of the rat. *J Neurophysiol.* 1994; 71:2046–2060. [PubMed: 7931501]
- Valentino RJ, Kosboth M, Colflesh M, Miselis RR. Transneuronal labeling from the rat distal colon: anatomic evidence for regulation of distal colon function by a pontine corticotropin-releasing factor system. *J Comp Neurol.* 2000; 417:399–414. [PubMed: 10701863]
- Vera PL, Nadelhaft I. Conduction velocity distribution of afferent fibers innervating the rat urinary bladder. *Brain Res.* 1990; 520:83–89. [PubMed: 1698508]
- Vizzard MA. Increased expression of spinal cord Fos protein induced by bladder stimulation after spinal cord injury. *Am J Physiol Regul Integr Comp Physiol.* 2000; 279:R295–305. [PubMed: 10896894]
- Wang HF, Shortland P, Park MJ, Grant G. Retrograde and transganglionic transport of horseradish peroxidase-conjugated cholera toxin B subunit, wheatgerm agglutinin and isolectin B4 from *Griffonia simplicifolia* I in primary afferent neurons innervating the rat urinary bladder. *Neuroscience.* 1998; 87:275–288. [PubMed: 9722157]
- Weaver LC, Cassam AK, Krassioukov AV, Llewellyn-Smith IJ. Changes in immunoreactivity for growth associated protein-43 suggest reorganization of synapses on spinal sympathetic neurons after cord transection. *Neuroscience.* 1997; 81:535–551. [PubMed: 9300440]
- Weaver LC, Verghese P, Bruce JC, Fehlings MG, Krenz NR, Marsh DR. Autonomic dysreflexia and primary afferent sprouting after clip-compression injury of the rat spinal cord. *J Neurotrauma.* 2001; 18:1107–1119. [PubMed: 11686496]
- Wilson P, Kitchener PD. Plasticity of cutaneous primary afferent projections to the spinal dorsal horn. *Prog Neurobiol.* 1996; 48:105–129. [PubMed: 8737440]
- Yoshimura N, Erdman SL, Snider MW, de Groat WC. Effects of spinal cord injury on neurofilament immunoreactivity and capsaicin sensitivity in rat dorsal root ganglion neurons innervating the urinary bladder. *Neuroscience.* 1998; 83:633–643. [PubMed: 9460769]
- Zagon A, Smith AD. Monosynaptic projections from the rostral ventrolateral medulla oblongata to identified sympathetic preganglionic neurons. *Neuroscience.* 1993; 54:729–743. [PubMed: 8332259]

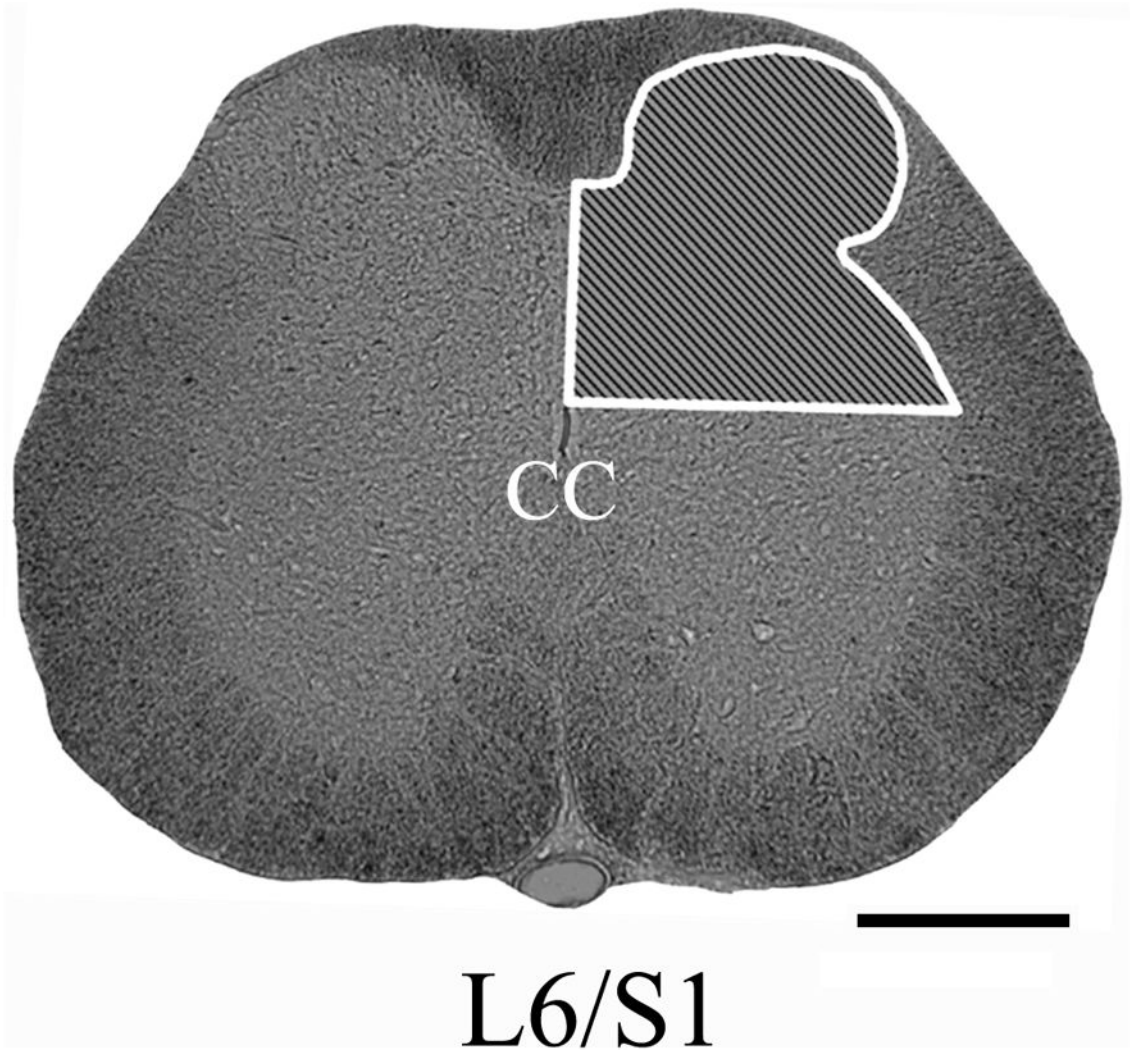


Fig. 1. Photomicrographs illustrating our region of interest for quantification (*shaded inset*) of CGRP⁺, RT97⁺, or CTb⁺ fiber density in the right upper dorsal gray matter at the L6/S1 spinal level. Scale bar=500 μ m. CC, central canal.

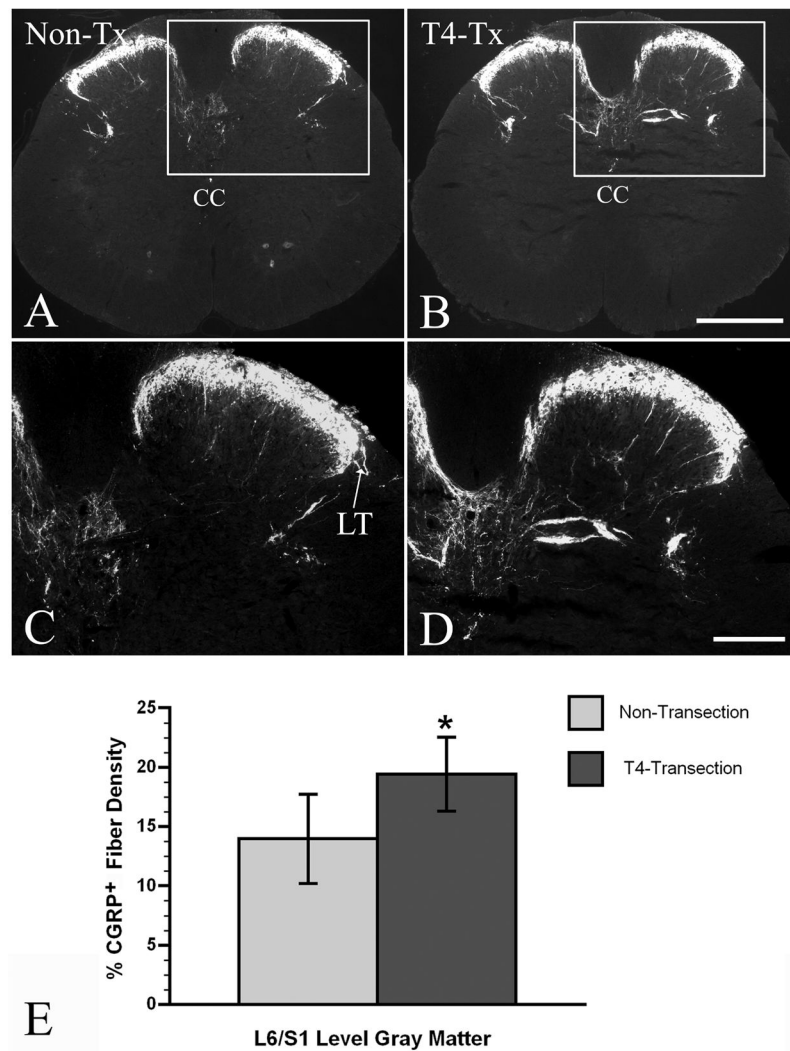


Fig. 2. Representative photomicrographs showing that, in both non-transected (Non-Tx) (**A**, **C**) and T4-transected rats (T4-Tx) (**B**, **D**), CGRP immunoreactivity was predominately expressed in the superficial dorsal horns including Lissauer's tract (LT), medial gray matter, as well as in the vicinity of the sacral parasympathetic nucleus (SPN) throughout the lumbosacral spinal cord. In most cases, the density of CGRP⁺ fibers appeared greater in transected spinal cords versus shams (**C** and **D** are high magnifications of boxed regions in **A** and **B**). Statistical analysis (**E**) demonstrated that the density of CGRP⁺ fibers in the L6/S1 spinal level was significantly greater in T4-transected (**B**, **D**) rats compared to shams (**A**, **C**) in the dorsal gray matter. Bars represent mean \pm SD. * $P < 0.05$, Scale bar = 500 μ m (**B**), 200 μ m (**D**). CC, central canal.

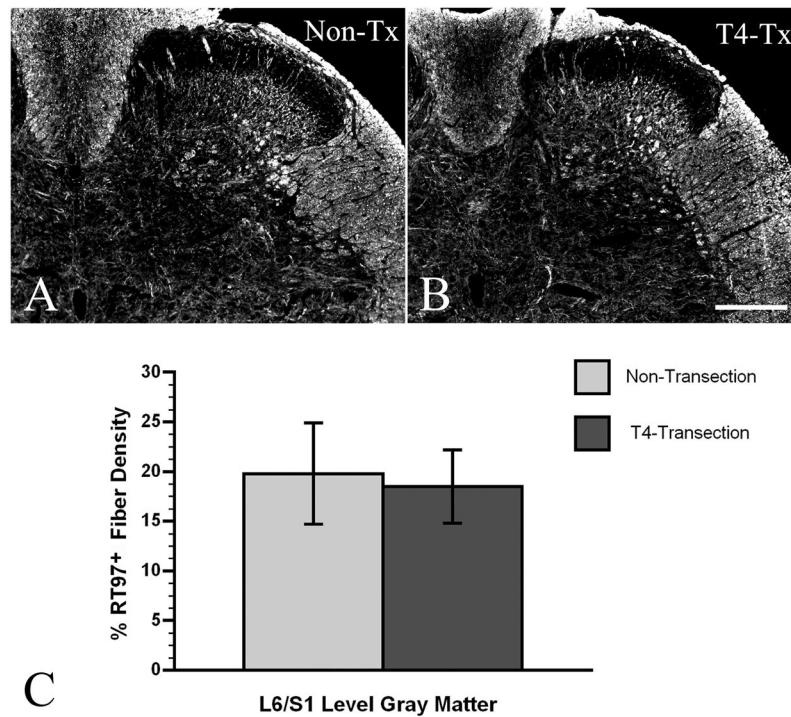


Fig. 3. Immunohistochemical staining for RT97 showing that positive fibers (Texas Red conjugated secondary antibody) were mainly distributed within laminae III–X in the gray matter, especially laminae III–V (A, B). Statistical analysis (C) showed that the density of RT97⁺ fibers was not significantly different at the L6/S1 spinal level between non-transected (Non-Tx) (A) and T4-transected (T4-Tx) (B) rats. Bars represent mean \pm SD. Scale bar=200 μ m.

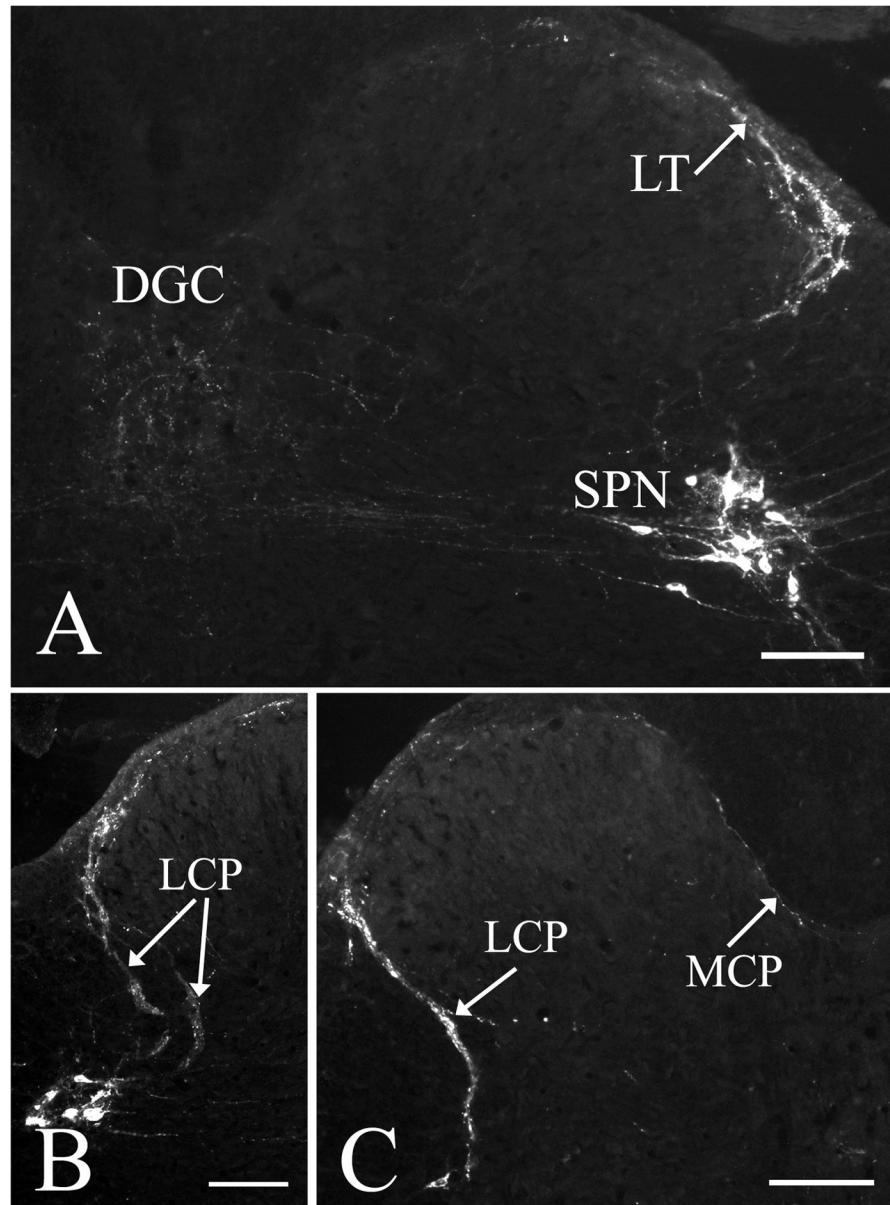


Fig. 4. Photomicrographs demonstrating that CTb-labeled colonic primary afferents in sham spinal cords are present in the Lissauer's tract (LT), laminae I–II, dorsal gray commissure (DGC) and sacral parasympathetic nucleus (SPN) (A). Labeled as well are the lateral collateral projection (LCP) (B, C) and the medial collateral projection (MCP) (C). Scale bars=100 μ m.

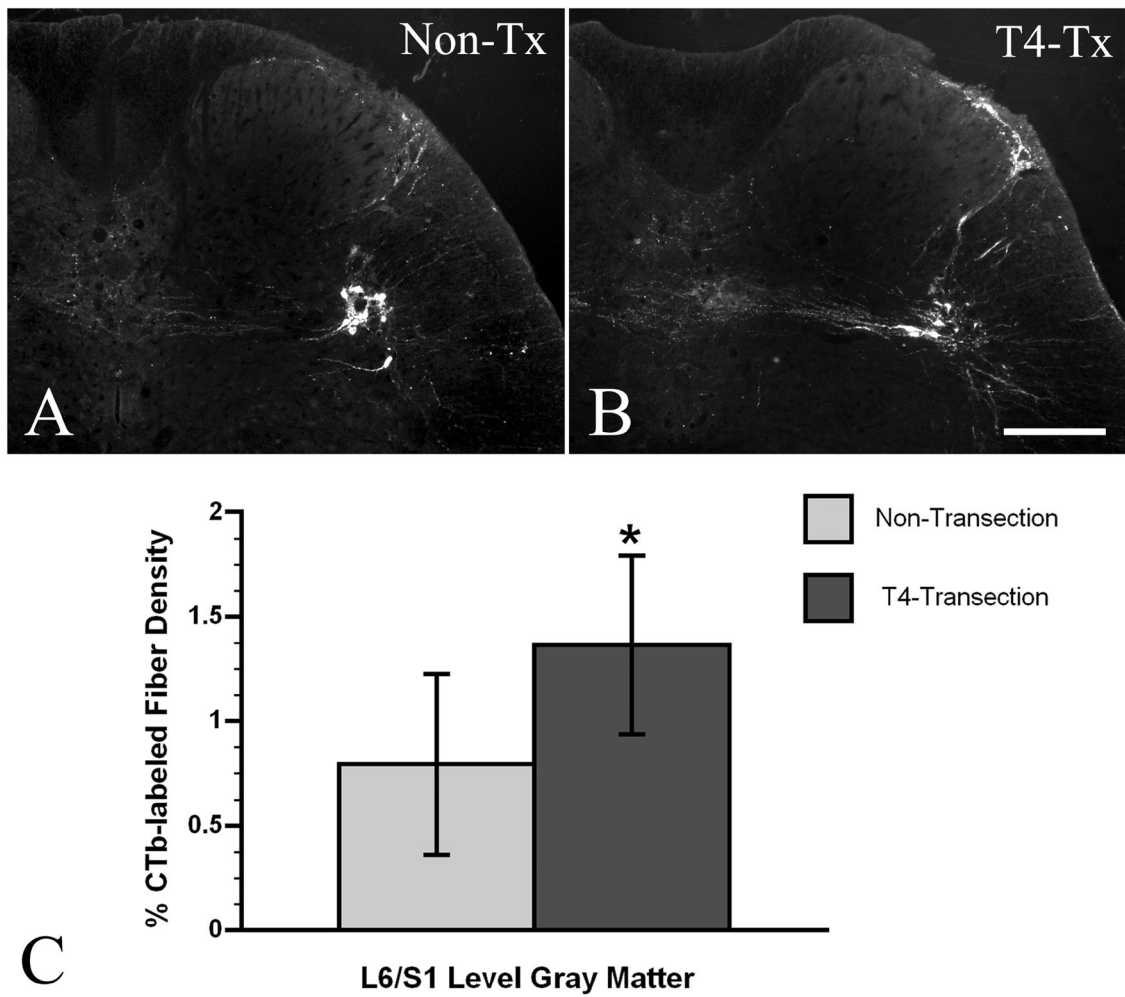


Fig. 5. Photomicrographs showing that CTb-labeled colonic visceral afferents at the L6/S1 level appeared greater in T4-transected (T4-Tx) spinal cords versus non-transected (Non-Tx) spinal cords (**A**, **B**). Statistical analysis (**C**) showed that the density of CTb⁺ fibers in the superficial dorsal horn was significantly increased following T4-transection. Bars represent mean ± SD. * $P < 0.05$, Scale bar=200 μ m.

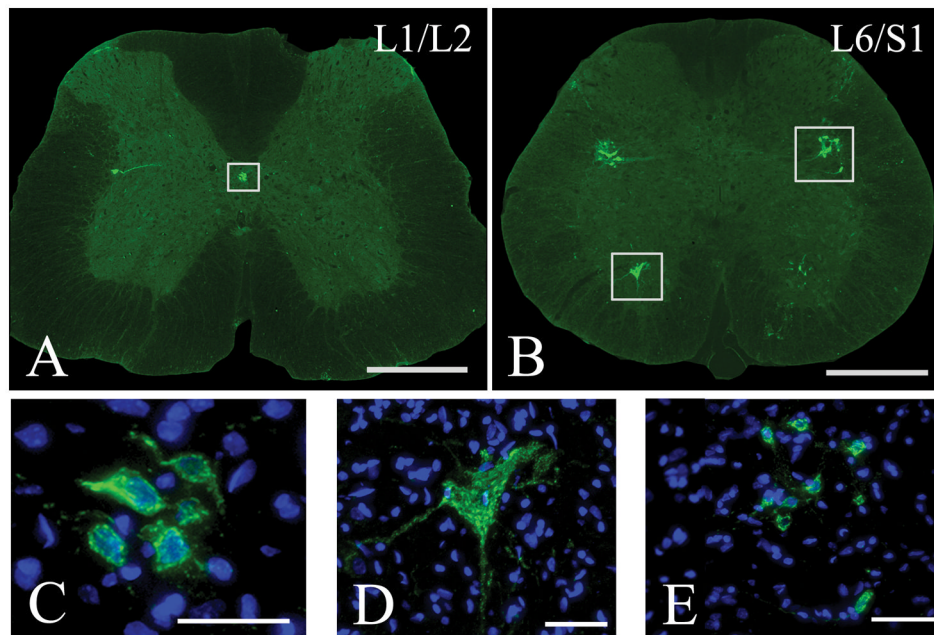


Fig. 6. Representative photomicrographs showing CTb-FITC labeling in sham spinal cords of animals injected with CTb into the distal colon. Panels **C**, **D**, and **E** are high magnification, Z-stacked confocal images of boxed regions in panels **A** and **B**, respectively, with Hoechst nuclear stain to identify individual cells. At the L1/L2 spinal level, CTb-labeled cell clusters were present in the DGC and, to a lesser extent, in the intermediolateral cell column (**A**, **C**). Throughout the thoracolumbar and lumbosacral segments, particularly at the L6/S1 spinal level, putative somatic motoneurons with large-diameter cell bodies were also labeled in the ventral horns (**B**, **D**). Note that the prominent CTb-labeled dendritic processes shown in **D** appear to emanate from two juxtaposed cells with distinct nuclei. In the contralateral ventral horn (**B**), however, the processes of a labeled cell not entirely within the plane of sectioning can be seen. Also, at the L6/S1 spinal level, CTb-labeled cells in the sacral parasympathetic nucleus (SPN) were prominent, bilaterally (**B**, **E**). Scale bars=500 μ m (**A**, **B**), 50 μ m (**C**–**E**).

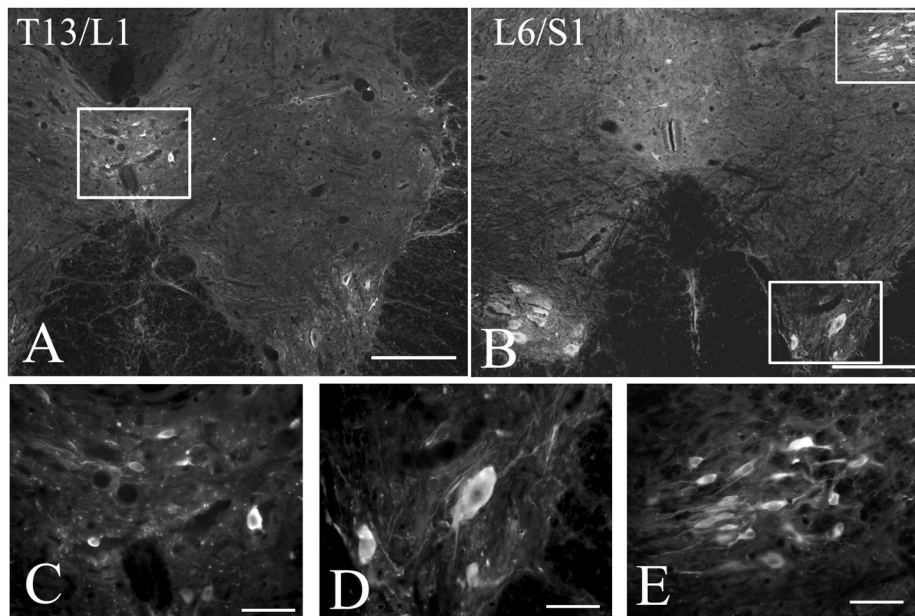


Fig. 7. Representative photomicrographs showing choline acetyltransferase (ChAT) immunolabeling in an adjacent slide series from sham spinal cords of animals injected with CTb. Panels **C**, **D**, and **E** are high magnifications of boxed regions in **A** and **B**, respectively. At the T13/L1 spinal level, ChAT-labeled cells were present in the DGC and the intermediolateral cell column (**A**, **C**). Throughout the thoracolumbar and lumbosacral segments, particularly at the L6/S1 spinal level, ChAT-labeled motoneurons with large-diameter cell bodies were present throughout the ventral horns (**B**, **D**), though with more frequency than CTb-labeled cells. Also at the L6/S1 spinal level, CTb-labeled cells in the sacral parasympathetic nucleus (SPN) were prominent, bilaterally (**B**, **E**). Scale bars=500 μm (**A**, **B**), 50 μm (**C**–**E**).

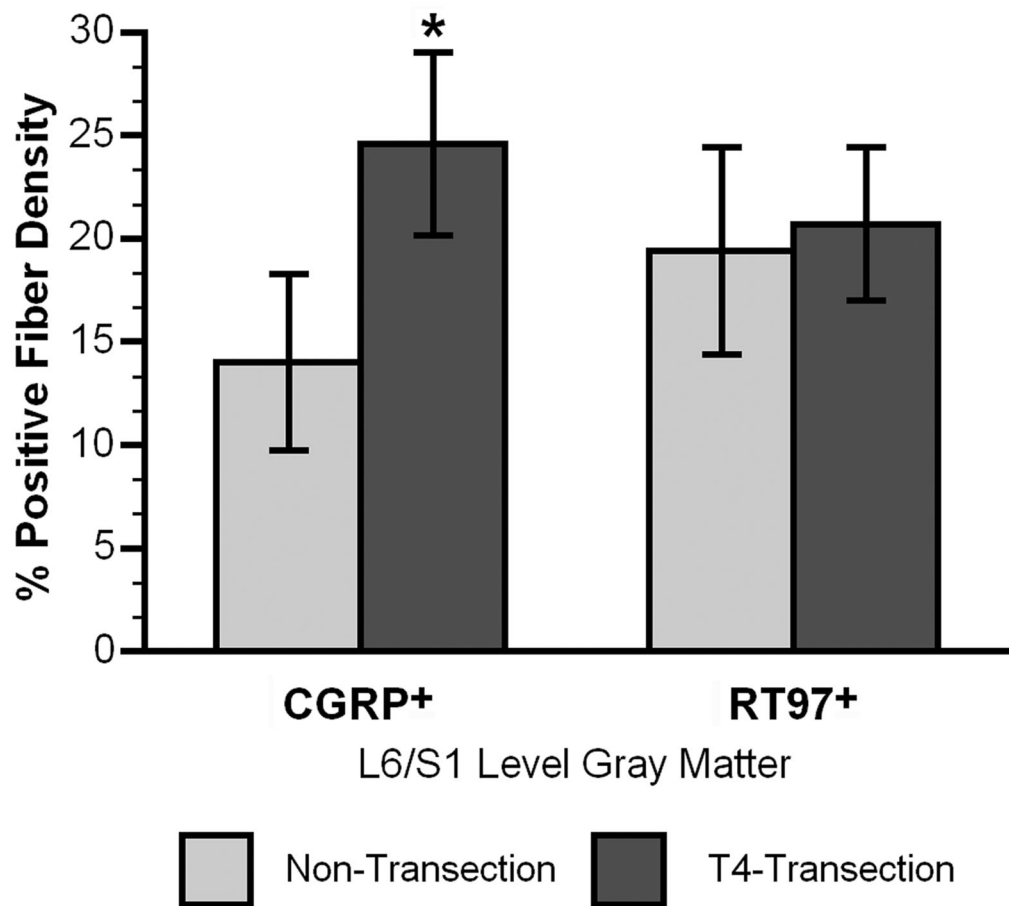


Fig. 8. Statistical analysis illustrates that spinal cord injury significantly increases the density of CGRP⁺ but not RT97⁺ fibers at the L6/S1 spinal level in the groups with CTb tracing. Bars represent mean \pm SD. * $P < 0.05$

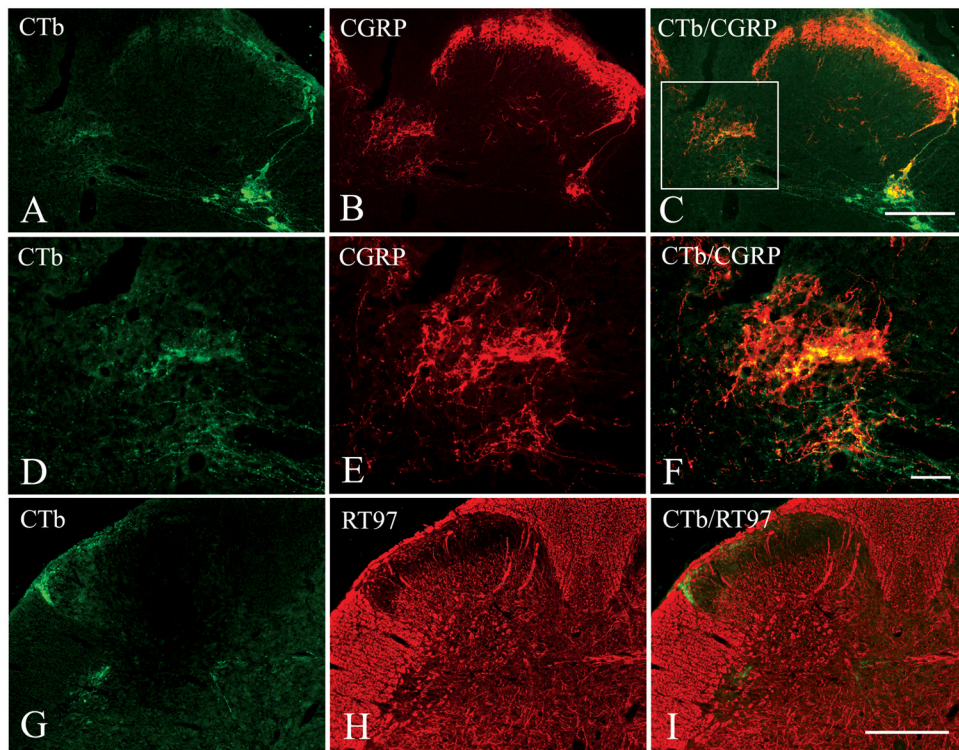


Fig. 9. Double immunofluorescent staining showing CTb-labeled colonic afferent fibers (FITC conjugated secondary antibody) (**A, D**) at the L6/S1 spinal level co-localized with CGRP⁺ pelvic afferents (Texas Red conjugated secondary antibody) (**B, E**) in Lissauer's tract, laminae I–II, dorsal gray commissure, as well as the sacral parasympathetic nucleus (**A–C**) in both non-transected and T4-transected spinal cords. **D, E, and F** are high magnifications of boxed regions in **C**. Double immunostaining for CTb⁺ colorectal afferents (**G**) and RT97⁺ fibers (Texas Red conjugated secondary antibody) (**H**) showed no co-localization (**I**). Scale bars=200 μm (**C, I**), 50 μm (**F**).

\$watermark-text

\$watermark-text

\$watermark-text

Table 1

Complete information and immunogen of primary antibodies applied

Antiserum	Species	Clonality	Working Dilution	Source Catalog/Lot Number	Immunogen
CTb	Goat	Polyclonal	1:1500	List Biological Laboratories, Campbell, CA 703/7032A5	Cholera toxin B subunit (choleraenoid)
CGRP	Rabbit	Polyclonal	1:2000	Sigma-Aldrich, Saint Louis, MO C8198/101K4846	CGRP-KLH
RT97	Mouse	Monoclonal	1:400	Chemicon, Temecula, CA CBL212/TR1418670	200 kDa neurofilament polypeptide
ChAT	Goat	Polyclonal	1:100	Chemicon, Temecula, CA ABI44P/0608037072	Choline acetyltransferase purified from human placental enzyme